ORIGINAL RESEARCH

Permeability-Enhancing and Protective Effect on Small Intestine of Punicic Acid in Different Forms and Their Nanoemulsions With Low Toxicity

Dongyan Duan[1,]*, Hua Xie[2,]*, Jiayi Jiang[1], Ping Yang[1], Zhiyuan Guo[2], Xiaoqiang Guo[1], Xingyu Chen[1], Qian Yao [1]

[1]Key Laboratory of Medicinal and Edible Plants Resources Development of Sichuan Education Department, Sichuan Industrial Institute of Antibiotics, School of Pharmacy, Chengdu University, Chengdu, 610106, People's Republic of China; [2]Sichuan Provincial Institute for Drug Control and Research, Chengdu, 610000, People's Republic of China

*These authors contributed equally to this work

Correspondence: Qian Yao, School of Pharmacy, Chengdu University, Shiling Town, Longquan District, Chengdu, Sichuan Province, 610106, People's Republic of China, Email yaoqian@cdu.edu.cn

Purpose: Most absorption enhancers boost the oral absorption of drugs via increasing intestinal permeability. However, they often damage intestinal mucosa and induce inflammatory reactions. The aim of this study is to synthesize a new absorption enhancer, punicic acid ethyl ester (PAEE), with excellent absorption-prompting effect and low toxicity.

Methods: The structure of PAEE was confirmed by NMR, MS, IR and UV. Setting oleic acid (OA) as the control, the three forms of punicic acid (PA), ie, free PA, PAEE, and pomegranate seed oil, in which PA exists in the form of triglyceride, were formulated into nanoemulsions (NE). The stability, physiochemical properties of the oils and NE were compared. The permeation-enhancing effect was estimated by phenol red intestinal transport experiments. The potential damage on small intestines was assessed by biochemical assay and pathological section.

Results: Though the three forms of PA had various strength in enhancing intestinal permeability, the difference was not significant ($p > 0.05$). Moreover, the effect was notably stronger than that of OA ($p < 0.05$) and was inversely related to the density and required HLB value of the oils. Compared to the corresponding oils, the NE exhibited much weaker effect in prompting intestinal permeability. Oral administration of OA and OA NE for 10 d impaired intestinal mucosa and villi along with strong inflammatory reactions in the small intestines. In contrast, the oils from PA series and their NE did not induce obvious intestinal inflammation. PAEE and its NE hindered the release of cytokines and increased the ratio of intestinal villus length to crypt depth.

Conclusion: PAEE is a promising absorption enhancer with a strong permeability-prompting effect and mucosa-protecting capacity against intestinal inflammation. It provides a practical strategy to enhance the bioavailability of the drugs with poor biological membrane penetration.

Keywords: punicic acid, punicic acid ethyl ester, pomegranate seed oil, nanoemulsions, permeability-enhancing effect

Introduction

Oral administration is the most popular administration route for drugs due to convenience and safety. However, many drugs have poor intestinal absorption and resultant low oral bioavailability. The utility of absorption enhancers is an efficient strategy to improve the oral absorption of the drugs.[1,2] Absorption enhancers include natural, semi-synthetic and synthetic substances, such as organic solvents, chelating agents, surfactants, endogenous bile salts, drugs (acetylsalicylic acid), polymers (polysaccharides), bacterial toxins, and so on. The use of absorption enhancers has been questioned for a long time due to safety and toxicity concerns.[3] The food additives with penetration-enhancing attribute, such as vegetable oils, medium and long chain fatty acids, bile salt (ie, sodium cholate), have gained special interest owing to the better safety.[4] For this reason, the vegetable oils and fatty acids were often used to assist the poorly permeable drugs to

Graphical Abstract
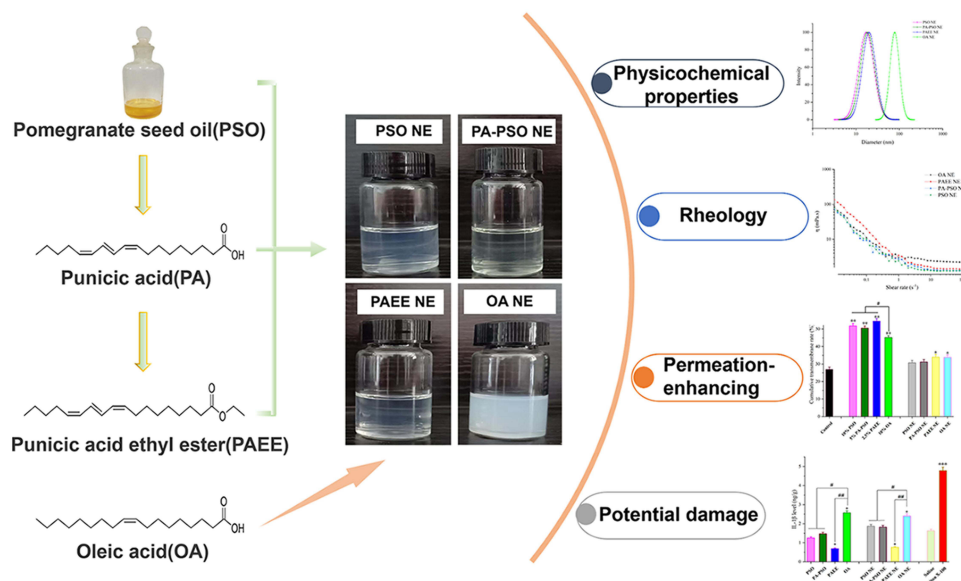
penetrate through biological membrane. For example, Lakshminarayana found that oleic acid (OA) and olive oil which was enriched in OA enhanced the intestinal accessibility of carotenoids more than linoleic acid and other vegetable oils.[5] Olive oil also enhanced the bioavailability and accumulation of lutein in lutein-deficient mice by modulating intestinal triacylglycerol lipase activity.[6] When adlay bran oil was administered concurrently with the probe drug, it increased the concentration of the probe drug and facilitated intestinal absorption of the drug.[7] When co-administered with edible oils or polyunsaturated fatty acid, the intestinal absorption of chlorogenic acid was increased.[8]

Our previous study revealed that pomegranate seed oil (PSO) prompted the transdermal diffusion of resveratrol.[9] PSO is obtained from pomegranate seeds which are discarded during pomegranate juice manufacture. The major fatty acid of PSO is punicic acid (PA), accounting for over 70% total fatty acids in PSO.[10] PA is a polyunsaturated fatty acid containing 18 carbons and three conjugated ethylene bonds,[11] possessing a higher degree of unsaturation than OA (18 carbons and one ethylene bond) and linoleic acid (18 carbons and two ethylene bonds). It was reported that the absorption-enhancing effect of a fatty acid increases with its unsaturation.[12] Thus, we assume that PA and PSO may have strong capacity to improve intestinal permeation.

Employing vegetable oils or fatty acid as the oil phase to formulate nanoemulsions (NE) is another commonly used strategy to enhance the oral absorption of drugs. In addition, NE have some other unique features, such as the capacity to load both hydrophilic and lipophilic drugs, augment the stability of encapsulated components, high thermodynamic stability, and so on.[13,14] Yin prepared baicalin NE by using hemp oil as the oil phase to improve the solubility and stability of baicalin. The oral bioavailability of baicalin NE was as high as 524.7% that of the baicalin suspension.[15] Sun used ethyl linoleate as the oil phase and prepared acetylpuerarin (AP) NE. After oral administration of AP NE to rats, the bioavailability of AP NE was 2.6-fold that of AP suspension.[16] In addition, NE can extend or enhance the effect of the encapsulated drug. The ketoprofen NE made from PSO showed the effect of reducing abdominal constrictions up to 12 h, whereas free ketoprofen maintained the effect only for 3 h.[17] Trans-resveratrol was entrapped into PSO self-nanoemulsifying drug delivery system (PSO SNDDS) and orally administered to the mice at a dose of 10 mg/kg. The swelling rate of mouse toes decreased by 40% compared to the free resveratrol group, manifesting more potent anti-inflammatory activity of PSO SNDDS.[18]

Fatty acids exist in vegetable oils in the form of triglycerides. Both fatty acids and vegetable oils can serve as an oil phase to prepare NE. All of them have absorption-enhancing capacity. One of the most important mechanisms for absorption enhancers to augment intestinal transport is to temporarily open the tight junctions of intestinal epithelial cells and increase the permeability of intestinal membrane.[19–21] The permeability-prompting attributes of fatty acids, vegetable oils and NE are closely associated with their physicochemical properties, which influence the interaction between intestinal membrane and absorption enhancers. Whether free fatty acids, vegetable oils, and their NE have different strength in interplaying with intestinal mucosa and changing its permeability, remains unclear. The oil or NE that is capable of significantly increasing intestinal permeability with negligible damage to the small intestines can be considered as a safe and efficient absorption enhancer, which is greatly needed for the drugs with poor oral bioavailability. Unfortunately, most of the absorption enhancers, including some natural fatty acids, will impair intestinal mucosa and induce inflammatory reactions. Thus, exploring new absorption enhancers that not only possess strong absorption-prompting capacity but also have low toxicity is very important in medical treatment.

Since PSO is derived from the daily fruit pomegranate, PSO and its principal fatty acid PA may have low biological toxicity. Like other fatty acids, PA exists in PSO in the form of triglycerides. Due to the presence of the conjugated double bonds, free PA is very unstable. In this study, two strategies were adopted to enhance PA stability: i) PA was dispersed in PSO which was abundant in flavonoids and polyphenols at the ratio of 1:1. ii) The carboxyl of PA was esterified by synthesizing PA ethyl ester (PAEE). Setting OA as a control, the physicochemical properties of PSO, PA in PSO (PA-PSO), PAEE and OA were examined comprehensively. The permeation-enhancing effect on small intestine of the three forms of PA, ie, triglyceride (PSO), ethyl ester (PAEE), and free form (PA-PSO), was compared. PSO, PAEE and PA-PSO can be employed as oil phase to prepare NE. As NE possess much larger surface area to contact with intestinal membrane, the penetration-enhancing ability of NE may be stronger than using oil alone. For this consideration, the NE were prepared, and the permeability-enhancing effect of the oils and NE from PA series was compared in this study as well. Moreover, how the physicochemical features of the oils and NE influenced their capacity to improve intestinal permeability was analyzed by principal component analysis (PCA). The potential damage of OA, PSO, PA-PSO, PAEE and their NE on intestinal mucosa was also assessed. Oral route is one of the most convenient administration modes in clinic. Considering large quantity of drugs has difficulty in transporting across small intestines, the utility of absorption-enhancers with high efficiency and low toxicity holds promising prospects in pharmaceutical fields.

Materials and Methods

Materials

The reference PAEE and the internal reference ethyl caprate were prepared by our lab with the purity of 95.86% and 98.75%, respectively, which were determined by GC using area normalization method. OA was purchased from Shanghai McLean Biochemical Technology Co., Ltd (Shanghai, China). Polyethylene glycol 400 (PEG 400) and 3.5-dinitrosalicylic acid (DNS) were obtained from Chengdu Kelong Chemical Reagent Company (Sichuan, China). Cremophor EL (EL) was purchased from Shanghai Aladdin Biochemical Technology Co., Ltd (Shanghai, China). Hematoxylin and eosin (H&E) dye was from Beyotime Biotechnology Company (Shanghai, China). Other reagents were of analytical grade and acquired from Chengdu Kelong Chemical Reagent Company (Sichuan, China).

Animals

Male Kunming mice were purchased from Chengdu Dossy Experimental Animals Co., Ltd. (Sichuan, China). Animal experiments were conducted following the guidance of Animal Care and Use of Chinese Good Laboratory Practice and approved by the Animal Research Committee of Chengdu University. The approval number for intestinal permeability test was SP221117 and for intestinal damage evaluation SP230512. The mice were adaptively raised for 3 d prior to the experiments with the cycle of 12 h daytime and 12 h night.

Preparation of PA and PA-PSO

The extraction of PSO and isolation of PA was carried out according to the method reported by Yang.[22] Briefly, PSO was extracted from pomegranate seeds with petroleum ether and under ultrasonic treatment. Subsequently, PSO was dissolved in a solution consisting of 3% potassium hydroxide (v/v) and 95% ethanol (v/v). The hydrolysis reaction was conducted at 85 °C for 30 min, and the pH was adjusted to 2.0 using hydrochloric acid. The fatty acid mixture was obtained by the extraction with petroleum ether, followed by the removal of the organic solvent via a RE-5203 rotary evaporation instrument (Yarong Biochemical Instrument Factory, Shanghai, China). PA was isolated from the fatty acid mixture using freeze-crystallization technology, based on its higher melting point. The purified PA was dispersed in PSO at the ratio of 1:1 (v/v) to obtain PA-PSO.

Synthesis of PAEE

PA of 25mg was mixed with 1 mL HCl-C_2H_5OH solution of 0.6 M and reacted under 70 °C water bath for 30 min. After the reaction was completed, ethanol and hydrochloric acid were removed under 55 °C by rotary evaporation. The product was loaded on a silica column and eluted with n-hexane, dichloromethane-hexane (2:3) and dichloromethane in turn. The fractions containing PAEE were combined, and the elution solvents were removed via rotary evaporation. The yield was 89.23% ± 2.16%.

Identification of PAEE

UV

The UV–vis spectrum was scanned by a UV2300 spectrophotometer (Techcom Co., Ltd., Shanghai, China) from 200 to 400 nm.

Fourier Transform Infrared Spectroscopy

The sample was mixed with KBr and compressed into a tablet. The Fourier transforms infrared (FT-IR) spectroscopy was scanned by a Two Infrared Spectrometer (PerkinElmer Co., Ltd., Massachusetts, USA) in the range of 4000 to 400 cm^{-1}.

GC-MS

GC-MS analysis was carried out on a Clarus SQ8 GC-MS instrument (PerkinElmer Co., Ltd., Massachusetts, USA). Sample separation was conducted on an HP-5 capillary column (30 m × 0.32 mm). Carrier gas was high-purity nitrogen with the flow rate of 1.5 mL/min. The injection was adopted split mode with the split ratio 20:1. MS detection adopted EI ion source with the temperature of 250 °C. The transfer line temperature was 300 °C with electron energy 70 eV and solvent delay 4 min. The molecules were scanned from 40 to 400 Da. The identification of fatty acids was performed using the MS database of the instrument software.

NMR

PAEE was dissolved in deuterated chloroform, and its ^{13}C-NMR and ^{1}H-NMR spectra were detected by a JNM-ECZ600R/S1 NMR spectrometer (JEOL, Tokyo, Japan).

Physicochemical Properties of Different PA Esters

Density, Refractive Index and Dielectric Constant

The oil of 1.0 mL was transferred to a beaker that had been dried to a constant weight. The weight of the oil was assayed accurately to acquire its density. A WAY-2WAJ Abbe refractometer (Shanghai YiCe Apparatus & equipment Co., Ltd., Shanghai, China) was used to determine the refractive index (RI) of the samples.

The electric capacity of air, n-hexane, and sample was measured by a simple parallel plate capacitor, respectively. The dielectric constant (DC) of the sample was calculated based on the following Eq (1):

$$D = (C - C_0)/(C_a - C_0) \times D_a \tag{1}$$

where D and D_a represent the DC of the sample and n-hexane, respectively. C, C_a and C_0 stand for the electric capacity of the sample, n-hexane and air, respectively.

The Required Hydrophilic Lipophilic Balance Value (HLB)

Tween 20 and Span 80 were blended together at different proportions to obtain the mixed emulsifiers with various HLB values. PSO, PA-PSO, PAEE and OA were emulsified by the mixed emulsifiers using the phase change temperature method, respectively.[23] After the turbidity of the emulsion was measured at 600 nm, the emulsion was centrifuged at 3000 r/min for 10 min, followed by the second measurement of the turbidity. The turbidity difference before and after centrifugation was calculated to assess the stability of the emulsion. The one with the least turbidity difference was considered the most stable emulsion, and the HLB value of its emulsifier was the required HLB (rHLB) of the oil phase. The formula for the calculation of rHLB value is shown in the Supplementary section.

Stability

PA, PA-PSO and PAEE were placed under 4 °C and room temperature, respectively. The PA content of the samples was determined by the GC method proposed by Yang et al on day 0, 10, 20 and 30, respectively.[22] The content on day 0 was set 100% and the data acquired on other days were compared with the content of day 0.

Preparation and Physicochemical Properties of NE

Preparation of NE

PSO, OA, PA-PSO and PAEE were employed as the oil phase to prepare NE, respectively, following the method reported by Lu et al.[18] EL and PEG 400 were selected as emulsifier and co-emulsifier, respectively. The oil phase, EL and PEG 400 were mixed together at the volume ratio of 1:4:4 and treated by ultrasound with a frequency of 400 hz for 10 min to guarantee the complete blending. Subsequently, 4 folds volume of distilled water was added dropwise under constant agitating at 600 r/min. The stirring was kept for another 30 min till the light blue color appeared, manifesting the formation of NE.[18]

Physicochemical Properties

The particle sizes, polydispersion index (PDI), and zeta potentials were measured by a ZEN 3600 Nanoparticle Sizer (Malvern Instruments Ltd., Worcs, UK). The rheological properties of the NE were determined by an MCR 302e rheometer (Anton Paar Company, Graz, Austria). All samples were run in two modes: i) rotational mode, where the viscosity was measured as a function of shear rate and shear stress ($0.01–100$ s^{-1}), and ii) oscillatory mode, where storage modulus (G′) and loss modulus (G″) were measured in the linear viscoelastic region as a function of strain (0.1%–10%) and frequency (0.05–2).

Stability in Gastrointestinal Fluids

Simulated gastric fluid (SGF) and intestinal fluid (SIF) were prepared according to the method proposed by Muszyńska et al.[24] The four NEs were diluted 10-fold with gastric fluid and intestinal fluid, respectively, and the particle sizes were determined immediately. Then, the NE solutions were placed in a SHZ-B thermostatic water shaker (Shanghai Boxun Medical & Biological Instrument Co., Shanghai, China) with the temperature set at 37 °C and the shaking speed at 50 r/min. The sizes of NE in gastric fluid were measured again after 2 h, and those in intestinal fluid were determined after 4 h.

The oils of PSO, PA-PSO, PAEE and OA at 2.5%, 5%, 10% were mixed with the intestinal fluid according to the proportion of 1:10 (v/v) to form the emulsions, respectively. The sizes were measured immediately. Afterward, the emulsions were incubated at 37 °C with the shaking speed of 50 r/min for 4 h. The sizes were assayed for the second time to examine the physical stability in intestinal fluid.

Permeability-Enhancing Effect of PA Esters and NE on Small Intestines

Processing Mouse Small Intestine

The male Kunming mice (14 weeks) were fasted but free access to water for 12 h prior to the experiment. Then, they were sacrificed by cervical dislocation. The small intestine was taken out from the lower part of the stomach.[25] After the inner contents were rinsed out with saline, the small intestines were maintained in saline of 37 °C for 1 h before use.

Intestinal Permeation of Phenol Red

The small intestines were filled with 1 mL PSO, PA-PSO, PAEE, and OA solutions of different concentrations as well as the corresponding NE containing 3.2% oil (v/v), respectively, and were incubated under 37 °C for 4 h. Subsequently, the samples were removed and replaced with 1 mL phenol red of 0.2 mg/mL. Then, the small intestines containing phenol red were immersed into 20 mL saline which was preheated to 37 °C and shaken at 50 r/min under 37 °C in a thermostatic shaker. At different time intervals, 0.5 mL solution outside the intestinal membrane was withdrawn, diluted with 1.5 mL distilled water, and the content of phenol red was determined using spectrophotometry at the wavelength of 558 nm.[25] Meanwhile, 0.5 mL saline of 37 °C was replenished into the release medium. Distilled water of 1 mL was set as the control and incubated with the small intestine for 4 h. The transmembrane process of phenol red was monitored as described above. The transport curves of samples were plotted using cumulative permeation rates versus time.

Potential Damage on Intestine

The mice, with the weight of 20 to 22 g, were randomly divided into 10 groups and each group included 5 mice. After adaptive feeding for 3 d, the mice were orally administered 10%PSO (v/v), 10%PA-PSO (v/v), 10%PAEE (v/v), 10%OA (v/v), and their NE at the dose of 1 mL/kg, respectively. The solutions containing oils were mixed intensively using a RTEX-5 vortex mixer (Haimen Kyin-Bell Lab Instruments Co., Ltd., Jiangsu, China) and were quickly withdrawn for the gavage. In addition, the experiment included a negative and positive control group that was orally administered saline and 3% Triton X-100 (v/v) at 1 mL/kg, respectively. The dosing was conducted twice daily and kept for 10 d consecutively. The mice were then fasted but free access to water for 12 h, followed by being sacrificed via cervical dislocation. The small intestines were removed from the mouse body, and the inner contents were carefully rinsed out with saline.

Cytokines in Mucosa Membrane of Small Intestine

The mucosa membrane of small intestine was weighed, homogenized with saline of 4 °C (1:6, w/w) and centrifuged at 10,000 r/min under 4 °C for 10 min.[26] The supernatant was subject to the determination of the levels of interleukin 1beta (IL-1β), interleukin-6 (IL-6) and tumor necrosis factor alpha (TNF-α) using commercial mouse ELISA kits (Shanghai Titan Scientific Co., Ltd., Shanghai, China).

Myeloperoxidase Activity

Intestinal myeloperoxidase (MPO) activity, a quantitative index of mucosal neutrophilic infiltrate, was measured conforming to what Menozzi et al proposed.[27] In brief, duodenum of 50 mg was homogenized with 1 mL hexadecyl-trimethylammonium bromide (HTAB) buffer (0.5% in 50 mm phosphate buffer, pH 6.0) and centrifuged at 10,000 r/min under 4 °C for 15 min. The supernatant of 7 μL was added to a 200 μL mixture which contained 0.167 mg/mL O-dianisidine dihydrochloride and 0.0005% hydrogen peroxide in 50 mm phosphate buffer (pH 6.0). The absorbance at 450 nm was determined by a ReadMax 1200 microplate absorbance reader (Shanghai Flash Spectrum Biological Technology Co., Ltd., Shanghai, China). The activity of MPO capable of degrading 1 μmol hydrogen peroxide per minute at 25 °C was assumed as one unit. Data were expressed as U/g tissue.

Sucrase Activity

The activity of sucrase was determined according to the method proposed by Zhang et al with some modification.[28] Briefly, duodenum of 25 mg was homogenized with 2 mL of 10 mm PBS (pH 6.1) of 4 °C, followed by centrifuging at 10,000 r/min for 10 min. The supernatant of 25 μL was blended with 50 μL PBS (20 mm, pH 6.9) and heated in the water bath of 37 °C for 10 min. Afterward, 1% sucrose (w/v) of 50 μL was added and reacted under 37 °C for another 30 min. Then, 100 μL DNS solution (0.55 g DNS and 27.83 g potassium sodium tartrate tetrahydrate were dissolved in 25 mL of 2 M sodium hydroxide) was added and reacted under 85–90 °C for 10 min. After the solution was cooled to room temperature, the absorbance at 540 nm was measured. The amount of glucose yielded by a sample was calculated via glucose standard curve.

Histological Change of Small Intestines

Histological changes were visualized by H&E staining. Briefly, the duodenum of a mouse was degreased, longitudinally cut, and rolled into a "Swiss roll". Slices with the thickness of 15 μm were obtained under −18 °C using a CM1860 cryosectioner (Leica Biosystems, Wetzlar, Germany) and were spread on glass slides, respectively. Then, the slices were fixed with 4% paraformaldehyde, stained with H&E, and gradually dehydrated by ethanol solutions. Finally, the sections were infiltrated with xylene and fixed by neutral balata. Histomorphology was observed under a BA410E microscope (Motic China Group Co., Ltd., Fujian, China) and scanned by an EASY SCAN 6 slice scanner (Motic China Group Co., Ltd., Fujian, China).

Statistical Analysis

The data were obtained from three parallel experiments and were expressed as the mean ± SEM. The difference among the groups was statistically analyzed by ANOVA and Turkey test, respectively. When $p < 0.05$, the difference was considered significant. Power analysis was carried out to examine if the sample sizes were statically adequate.

Two groups of data were processed PCA: i) the penetration rate of phenol red at the optimal oil concentration versus the physical attributes of corresponding oil, and ii) the permeation rate of phenol red across the small intestine pre-incubated with NE versus the physical properties of NE. Data were input to SPSS 19.0 software ((IBM, Armonk, NY) and standardized. Meanwhile, dimension reduction was conducted. Principle components (PC) were determined according to the contribution to the total variance. The correlations between penetration rate and physical properties were assessed based on the array table created by the software.

Results

Identification of PAEE

UV and IR

The UV and IR spectra of PAEE and PA are shown in Figure S1. In the UV spectra, either PAEE or PA had three distinct absorption peaks around 270 nm. The maximum absorption wavelength was at 278 nm with two shoulder peaks at 273 and 284 nm.[29,30] It indicates that after the esterification, the double bonds of PA were not broken and still present in PAEE.

In the IR spectra of PA, the peak at 3310 cm^{-1} was yielded from the hydroxyl stretching vibration of carboxylic acid.[31] PAEE had a weak and characteristic peak at 3449.59 cm^{-1}, which was assigned to the dimer carbonyl of ester.[32] In addition, PA had a peak at 1713.15 cm^{-1}, which was derived from carbonyl stretching vibration of carboxylic acid.[31] In comparison, the carbonyl stretching vibration peak of PAEE appeared at 1732.89 cm^{-1} with stronger intensity.[33] The peaks of 1181 and 1031 cm^{-1}, representing the asymmetric and symmetric stretching vibration of ester, were also present in the spectrum of PAEE, but were absent in the spectrum of PA.[33] According to the above analysis, it can be determined that PAEE was formed.

GC-MS

The total ion chromatogram (TIC) of purified sample as well as the MS of the PAEE (peak 6) is displayed in Figure 1A. The molecular ion peak of m/z 306 was exactly the molecular weight of PAEE. Besides, other characteristic peaks belonging to PA, for example, *m/z* 55, 67, 79, 108, 121, 135, 149, and so on,[34] were also present in the MS, verifying the successful synthesis of PAEE.

NMR

The ^{1}H NMR and ^{13}C NMR spectra of PAEE and PA are shown in Figure 1B and C. The ^{1}H NMR of the synthesized compound is very similar to that of PA. The signal peaks of *trans*-CH=CH- at 5.41 ppm and *cis*-CH=CH- at 6.03 and 6.45 ppm were also present in the ^{1}H NMR of PAEE, confirming that the configuration of PA was well retained in PAEE.[35,36] In addition, the ^{1}H NMR of PAEE included 4.11 ppm (2H), which was assigned to the hydrogen that was connected with oxygen atom of ester group.[37] In the ^{13}C NMR, apart from the peaks from PA, PAEE contained the peak
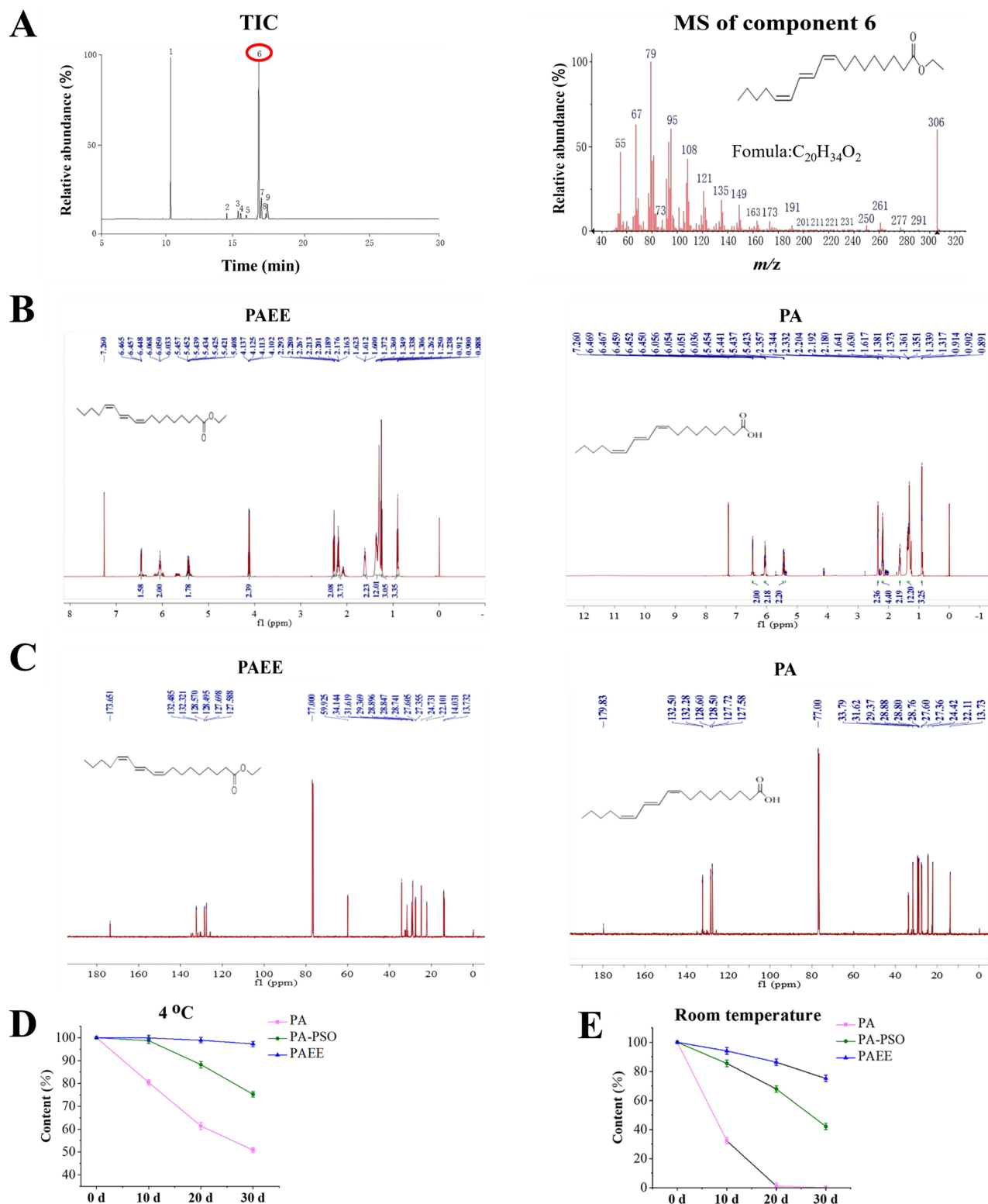
Figure 1 Identification of PAEE: (**A**) TIC of the sample and MS of peak 6. (**B**) ^{1}H-NMR of PAEE and PA. (**C**) ^{13}C-NMR of PAEE and PA. (**D**) Stability of the oils at 4°C. (**E**) Stability of the oils at room temperature (20–25°C).

Notes: 1. ethyl decanoate (internal standard); 2. ethyl palmitate; 3. ethyl linoleate; 4. ethyl oleate; 5. ethyl stearate; 6. PAEE; 7–9: three isomers of PAEE.

Abbreviations: TIC, total ion chromatogram; PA, punicic acid; PAEE, punicic acid ethyl ester.

at 59.92 ppm derived from the carbon linking with the oxygen atom of ester group.[37] The difference indicates that the ethyl ester was successfully synthesized in PAEE.

Physicochemical Properties of Different PA Esters

Physicochemical Properties
The physicochemical parameters of PSO, PA-PSO, PAEE, and OA are shown in Table 1. The density order was OA>PSO>PA-PSO>PAEE. PSO had the highest DC among the four oils, followed by PA-PSO. The DC of PAEE was the lowest. RI exhibited the similar trend as DC, but the variations were relatively small. PAEE presented the lowest rHLB. The rHLB of the other three oils diminished with the increase in the DC.

Stability
The stability of the oils under 4 °C and room temperature is shown in Figure 1D and E. Compared to PA and PA-PSO, PAEE presented the highest stability, able to maintain stability for over one month at 4 °C. When PA was dispersed in PSO, the stability was also improved. However, when maintained at room temperature for 30 d, the oils from PA series were degraded to various degrees. The stability order was PAEE>PA-PSO>PA.

Physicochemical Properties of NE From PA Esters

Sizes and Potentials
The appearance and size distribution of NE are displayed in Figure 2A. The particle size of OA NE was around 76 nm, while the diameters of the other three NE were around 20 nm. The PDI of all NE was less than 0.3, indicating the uniform size distribution. All NE exhibited zeta potentials ranging from −6 to −3 mV, indicating that they are approximately electrically neutral. After being placed at room temperature for 3 months, the sizes, PDI and zeta potentials of all NE slightly increased, manifesting the good physical stability.

Stability in Gastrointestinal Fluids
The stability of NE in gastrointestinal fluids is presented in Figure 2B. Being placed in gastric fluid for 2 h, only OA NE had 29.46%±3.18% diameter increment. The sizes of other NE kept invariable. In addition, the gastric fluid inverted the zeta potentials of the NE from negative to positive. However, the values were very small. The diameter of PSO NE increased 25.43%±2.38% after incubation in intestinal fluid for 4 h, while the other NE maintained stable. Meanwhile, intestinal fluid augmented the net negative potentials of the NE from −6 to around −20 mv, which increased the repulsive force among the particles, and prevented the aggregation of NE in small intestine.

When the oils were diluted with intestinal fluid, the emulsions were developed, and the size changes after the incubation at 37 °C for 4 h are shown in Figure 2C. It manifests that the diameters of droplets rose with the increment of oil concentration. The sizes of emulsions produced by 10% PSO and 10% OA were beneath 140 nm, whereas PA-PSO and PAEE of 10% (v/v) yielded the emulsions with the diameters over 150 nm after the incubation, implying that the emulsions from 10% PA-PSO or 10% PAEE may have smaller total surface area.

Table I Physicochemical Properties of the Oils (n = 3)

Parameters	PSO	PA-PSO	PAEE	OA
Density (g/mL)	0.8823±0.0209	0.8801±0.0217	0.8731±0.0182	0.8889±0.0124
RI	1.493±0.028	1.492±0.022	1.483±0.013	1.488±0.024
DC	3.182±0.034	2.507±0.051	2.179±0.023	2.361±0.021
rHLB	12.50±0.24	14.30±0.07	11.30±0.10	16.70±0.16

Abbreviations: PSO, pomegranate seed oil; OA, oleic acid; PA-PSO, punicic acid dispersed in pomegranate seed oil (1:1, v/v); PAEE, punicic acid ethyl ester; RI, refractive index; DC, dielectric constant; rHLB, required hydrophilic lipophilic balance.
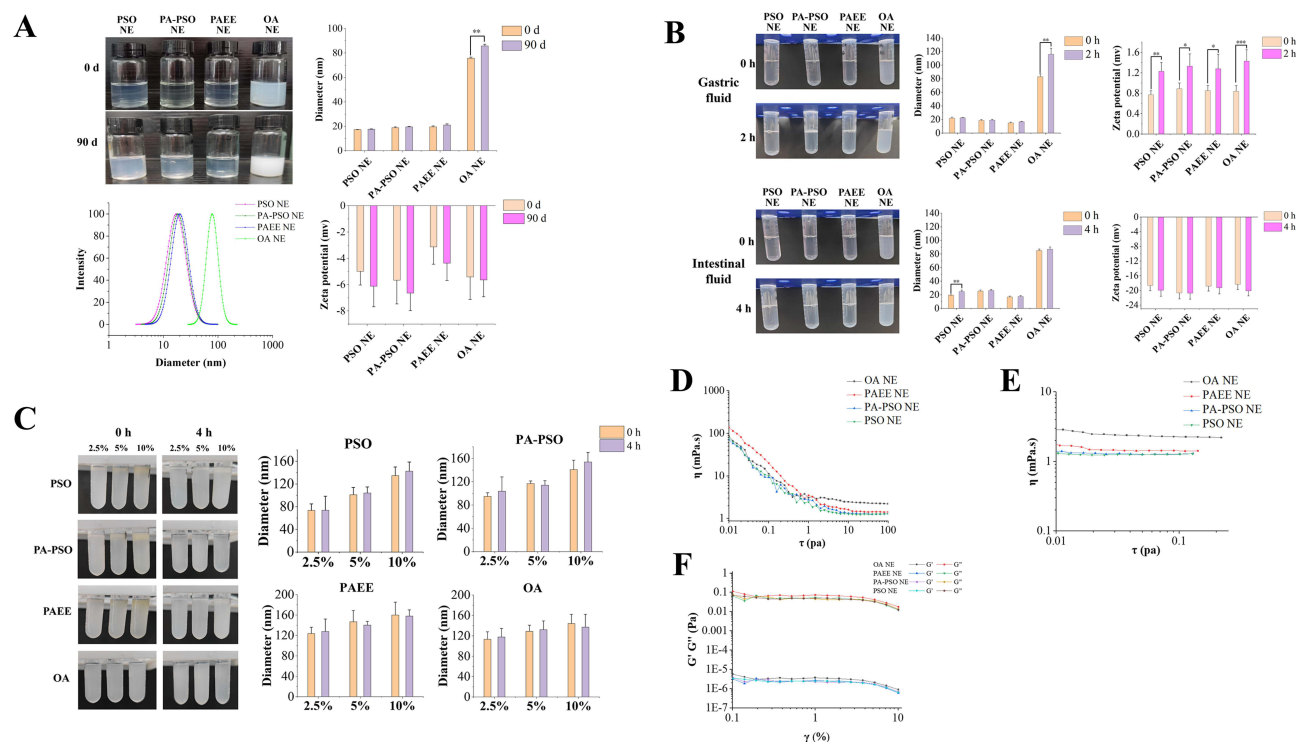
Figure 2 The appearance, particle size, and the changes in diameter and zeta potential of the NE and emulsions: (**A**) NE were stored at room temperature (20–25°C) for 3 months. (**B**) NE were incubated under 37 °C with gastric acid for 2 h, or with intestinal fluid for 4 h. (**C**) Emulsions developed by the oils were incubated with intestinal fluid under 37 °C for 4 h. (**D**) NE viscosity as function of shear rate. (**E**) NE viscosity versus shear stress. (**F**) NE modulus as function of strain (γ%). *, **, ***p<0.05, p<0.01, and p<0.001.

Abbreviations: NE, nanoemulsions; PSO, pomegranate seed oil; PA-PSO, PA dispersed in PSO at 1:1 (v/v); OA, oleic acid. Other abbreviations are as Figure 1.

Rheological Properties

Figure 2D shows that the four NE had shear thinning behavior and viscosity decreasing with the elevation of shear rate. Moreover, when the shear rate was greater than $10s^{-1}$, the network structure of the system was completely destructed, and the apparent viscosity remained unchanged. Stress had no discernible impact on the viscosity of NE (Figure 2E), exhibiting the typical characteristic of pseudoplastic fluid.[38] OA NE exhibited obviously higher viscosity than the NE of PSO series. Among the three NE derived from PA, the viscosity of PAEE NE was the highest.

The oscillatory shear measurements were carried out, and the results are shown in Figure 2F. It shows that the G′ values of the NE were very low (below 0.001 Pa), and the G″ values were significantly higher than G′ throughout the strain range, suggesting that no gelling occurred in the process.

Permeation-Enhancing Effect of PA Series and Their NE on Mouse Intestinal Membrane

Permeation of Phenol Red Across Mouse Small Intestine

The membrane permeation curves of phenol red are shown in Figure 3A to D. Around 27% of phenol red permeated through mouse small intestine. Both the oils and their NE improved the permeability of small intestine to varying degrees. The penetration-enhancing strength of PSO and OA showed a concentration-dependent manner. The transmembrane amount of phenol red increased with the elevation of oil concentrations. Conversely, PAEE presented the opposite trend that the permeation amount declined with the increase of PAEE concentration. Meanwhile, the strongest permeation-enhancing strength of PA-PSO was obtained by 5% concentration (v/v), followed by 10% concentration (v/v).

The maximum cumulative transmembrane rates of phenol red at the optimal oil concentration and the permeation rates of NE are displayed in Figure 3E. It is noteworthy that compared to the absorption of phenol red with OA, the permeation of phenol red aided by PSO, PA-PSO and PAEE increased 20%, verifying the more potent permeation-
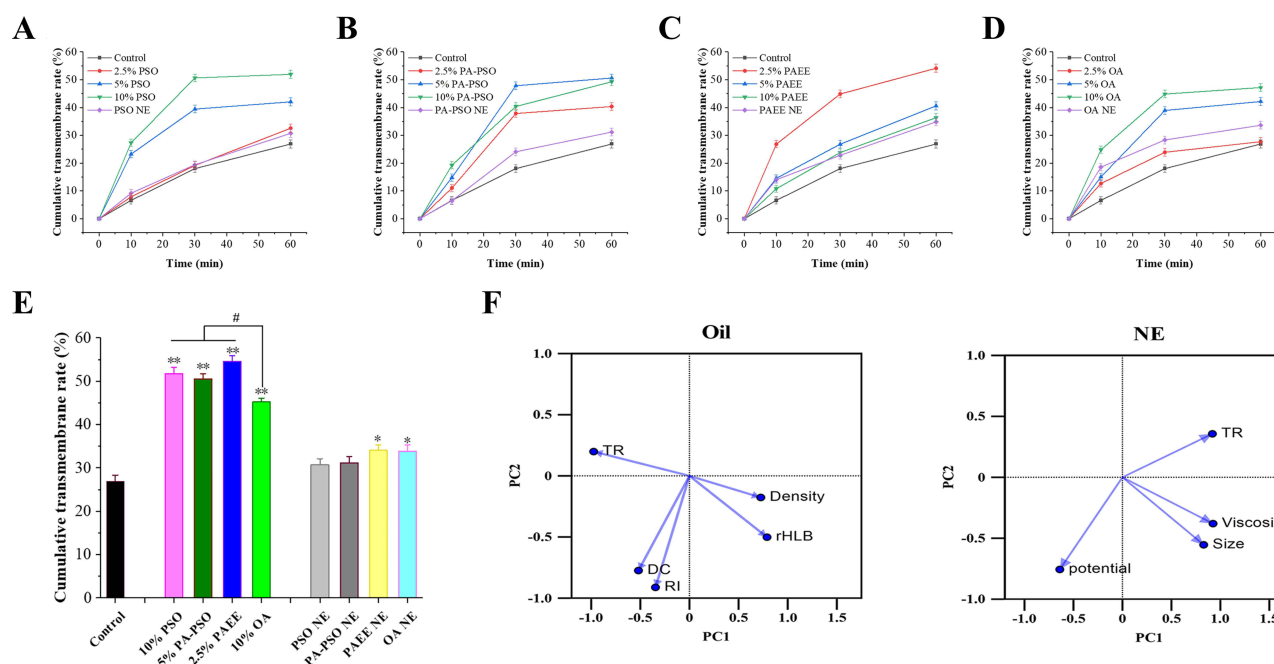
Figure 3 Transmembrane curves of phenol red with PSO and PSO NE (**A**), PA-PSO and PA-PSO NE (**B**), PAEE and PAEE NE (**C**), OA and OA NE (**D**), the comparison of the maximum cumulative transmembrane rates (**E**), and principal component analysis of transmembrane rates and physicochemical properties of the oils and their NE (**F**). *, **: p<0.05 and p<0.01, compared with the control group. #p<0.05. Power analysis confirmed that the sample sizes were statistically adequate.
Abbreviations: RI, refraction index; DC, dielectric constant; TR, transmembrane rate. Other abbreviations are as Figure 1 and 2.

enhancing strength of the oils belonging to PA series. The penetration with PSO, PA-PSO and PAEE varied with each other, but the difference was not obvious ($p > 0.05$). The cumulative permeation amount of phenol red with NE was only 50% to 70% that of the oil at optimal concentration, manifesting that oil has stronger penetration-enhancing strength than the corresponding NE. Although the permeability-prompting effect of OA was significantly weaker than that of the oils from PA series, OA NE presented better permeability-enhancing power on small intestine, but the difference was not significant ($p > 0.05$). It implies that the oil phase contributed little to the effect of the NE.

PCA

The maximum permeation rates of phenol red at the optimal oil concentration and the physicochemical properties of the oils were subjected to PCA. The array in factor analysis shows that transmembrane rate (TR) of phenol red was negatively correlated with the density ($r = -0.791$) and rHLB ($r = -0.902$) of oil. It means that the oil with low density and small rHLB will have a stronger effect in enhancing the permeability of small intestine. Two PC were extracted to represent the parameters, accounting for 85.31% of total variance. The PC diagram is displayed in Figure 3F. TR, rHLB and density were loaded onto PC1, standing for the penetration-enhancing capacity of oil. RI and DC were loaded onto PC2, representing oil polarity.

The permeation-enhancing effect as well as the physical properties of NE were input as the parameters for PCA. The array shows that TR of NE was positively related to the viscosity ($r = 0.737$) and negatively correlated with the zeta potential ($r = -0.833$). Two PC were selected to represent the attributes of NE, occupying 98.65% of total variance. TR, viscosity and size, which were associated with NE fluidity, were loaded onto PC1. Zeta potential was loaded onto PC2, standing for the electrical property of NE.

Potential Damage on Small Intestine
Cytokines in Mucosa Membrane of Small Intestine
The cytokine levels in small intestines are shown in Figure 4A to C. The group of positive control Triton X-100 triggered large amounts of cytokines to be released in small intestine. Compared to saline group, the administration of PAEE and its NE reduced IL-1β level in small intestine by 57.93%±0.74% and 53.51%±0.95%, respectively, whereas OA and OA
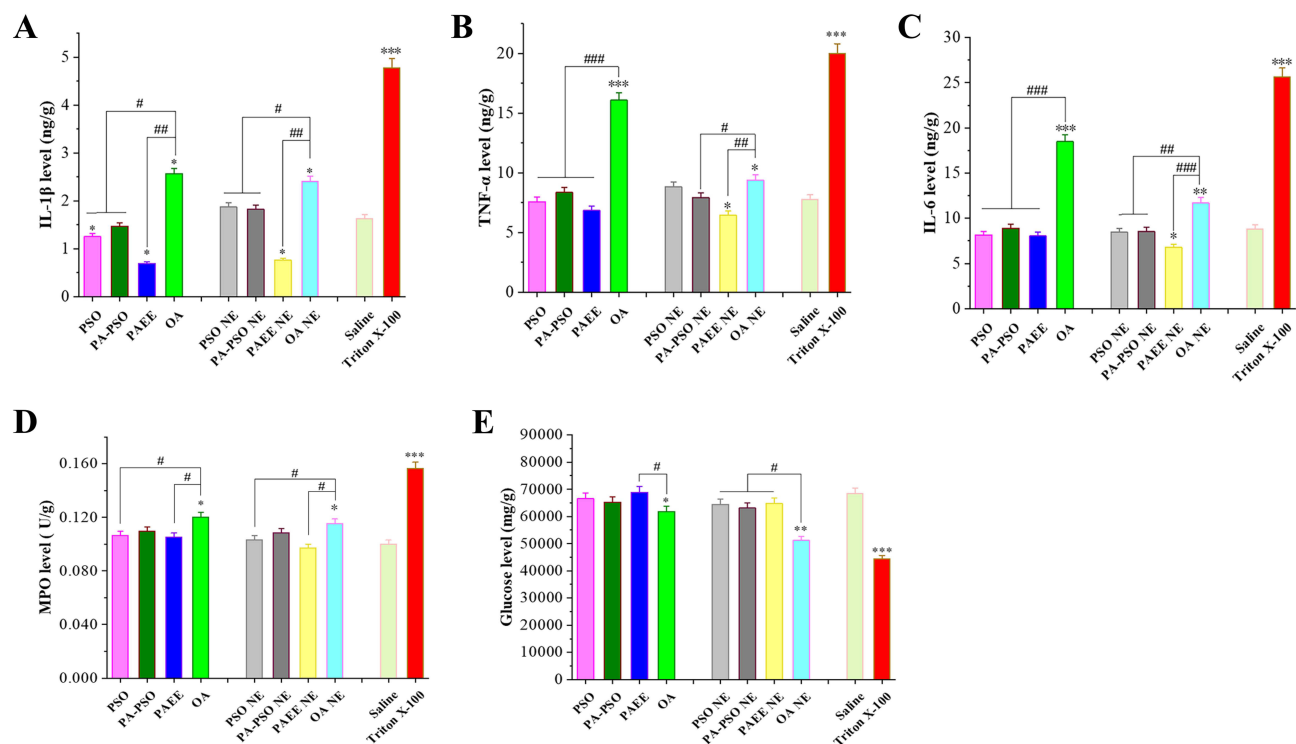
Figure 4 The levels of IL-1β (**A**), TNF-α (**B**), IL-6 (**C**), MPO activity (**D**), and sucrase activity (**E**) in small intestines of mice after oral administration for 10 d. *, **, ***$p<0.05$, $p<0.01$, and $p<0.001$, compared with the group of saline. #,##,###: $p<0.05$, $p<0.01$, and $p<0.001$. Power analysis confirmed that the sample sizes were statistically adequate.

NE increased IL-1β level by 58.31%±1.13% and 47.60%±1.18%, respectively. The application of PSO and PA-PSO decreased the level by 19.27%±1.05% and 7.08%±0.86%, respectively (Figure 4A). However, PSO NE and PA-PSO NE slightly elevated IL-1β concentration by 12.52%±2.13% and 6.25%±1.57%. The groups of oils from PA series and their NE presented notably lower IL-1β concentrations than OA and OA NE group ($p < 0.05$).

With respect to saline group, Triton X-100, OA and OA NE increased TNF-α level in the small intestine by 157.65% ±6.13%, 107.08%±3.95% and 20.59%±1.12%, respectively, manifesting that Triton X-100 and OA triggered serious inflammatory reaction (Figure 4B). In contrast, PAEE and PAEE NE lowered the level by 11.84%±1.66% and 16.73% ±1.43%. In the oil and NE groups from PA series, only PA-PSO and PSO NE elevated the level by 7.72%±0.66% to 13.38%±0.91%. The TNF-α levels induced by the oils from PA series were much lower than that triggered by OA ($p < 0.001$).

Compared to saline group, Triton X-100, OA and OA NE increased IL-6 level by 190.69%±7.44%, 109.88%±4.16% and 33.03%±2.82%, respectively. The oils and NE from PA series did not trigger the release of IL-6. PAEE NE decreased IL-6 concentration by 8.63%±0.77% (Figure 4C).

MPO Activity

Intestinal MPO activity of different groups is shown in Figure 4D. Compared to saline group, the MPO activity of the groups of Triton X-100, OA and OA NE increased 56.50%±3.51%, 20.10%±1.18% and 15.30%±1.03%, respectively, indicating the occurrence of inflammation and infiltration of neutrophils. Other groups slightly augmented the enzyme activity but had no significant difference with saline group ($p > 0.05$).

Sucrase Activity

Intestinal sucrase activity of different groups is displayed in Figure 4E. Compared to saline group, the glucose level of Triton X-100, OA and OA NE group was decreased 51.36%±3.56%, 9.31%±1.02% and 13.12%±1.18%, implying the serious impairment of small intestine induced by Triton X-100. With respect to saline group, the oils from PA series

presented small variation in glucose level without statistical difference (p > 0.05). The corresponding NE reduced glucose level by 5.28% to 7.71%, which was substantially lower than that of OA NE (p < 0.05). It implies that both the oils and NE of PA series did not bring obvious unfavorable impact on the sucrase of small intestines.

Intestinal Histomorphology

The small intestinal histomorphology is shown in Figure 5A. Compared to the normal saline group, the villus structure of Triton X-100 group was almost destroyed with shortened length and scattered debris. OA group presented a partially impaired villus structure. Some villi deformed and the muscle layer became thinner. OA NE group maintained a relatively complete villus structure. However, the villus wall was damaged and looked rough. The mucosa morphology was in consistent with the degree of inflammation (Figure 4A to C). The oil groups from PA series exhibited regular villus structure with normal or increased length. The NE of PA series preserved intact villus morphology. However, slight lesion in the wall was observed in the groups of PSO NE and PA-PSO NE. Only PAEE NE group retained smooth outer wall of villi.

The villus length and crypt depth were measured from 6 different segments, respectively. The ratios of villus length to crypt depth were calculated and shown in Figure 5B. Compared to saline group, the ratios of Triton X-100, OA and OA NE group were reduced 51.78%±4.13%, 31.04%±2.82% and 24.31%±2.88%, respectively, implying the damage of intestinal mucosa. The oils from PA series slightly increased the ratio, presenting the protective effect on small intestines. Notably, the ratio of PAEE group rose 17.42%±1.16%. PSO NE and PA-PSO NE group decreased the ratio by around
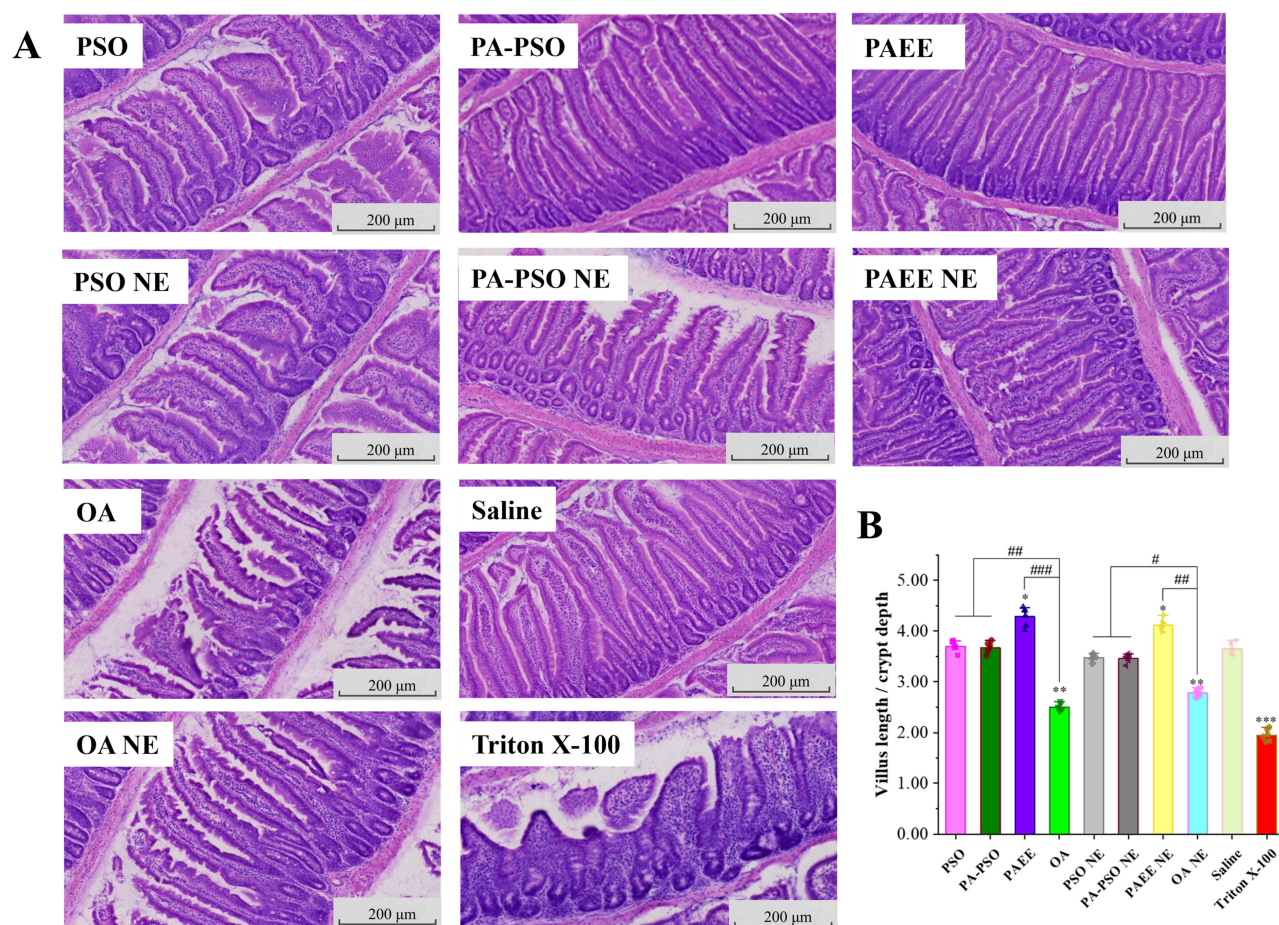

Figure 5 The small intestinal histomorphology by H&E staining (**A**), and the ratios of villus length to crypt depth (**B**) of different groups. *, **, ***p<0.05, p<0.01, and p<0.001, compared with the group of saline. #,##,###p<0.05, p<0.01, and p<0.001. Power analysis confirmed that the sample sizes were statistically adequate.

6%, while PAEE NE elevated the ratio by 11.11%±1.23%, manifesting the distinctive low toxicity of PAEE NE via oral administration.

Discussion

The molecule with high dipole moment is categorized into polar molecule, and the DC it generates is usually high. RI, representing the passing velocity ratio of light through air to through a medium, is positively related to the clarity of medium. In addition, RI increases with the number of double bonds.[39] A molecule including more double bonds has fewer hydrogen atoms and lower molecular weight, making the molecule easily aligned with the electric field, which in turn leads to an increase in the DC.[40] This study also affirms that RI increases with DC. In comparison, the polarity differences among components can be reflected by DC more clearly.

The rHLB represents the most suitable emulsifier that can strongly interact with the oil, co-emulsifier and water, and form the smallest droplets. The emulsifier with higher HLB is usually used to emulsify the oil with higher RI.[41] However, in this study, except PAEE, the rHLB decreased with the elevation of RI. The possible reason is that the four oils had relatively high polarity with the RI over 1.485. The polar fraction endowed the oil with amphiphilic character and relatively better compatibility with water. As a result, rHLB for emulsifying polar oil decreased.

PA is very unstable. However, when it was dispersed in PSO (PA-PSO) or esterified into PAEE, its stability was increased dramatically. The three conjugated double bonds present in PA structure are responsible for the instability of PA. In addition, free PA has a carboxyl, which increases the polarity of the molecule as well as the chance of interacting with water and radicals, leading to the degradation of PA under high humidity or upon the attack of free radicals. The esterification of PA reduced the attack from polar molecules such as water and radicals and improved the stability of the compound. PSO is abundant in natural antioxidants, such as polyphenols and flavonoids,[42,43] which well protect PA from degrading.

Though the sizes of all NE were beneath 100 nm, the diameter of OA NE was obviously larger than the NE of PA series. The four NE were prepared using the same formula for the comparison purpose. EL was selected as the emulsifier with HLB 11.3, which was close to rHLB of PSO, PA-PSO, and PAEE, but much lower than that of OA. For this reason, OA NE produced the greater size. To confirm this viewpoint, Tween 20 with the HLB 16.7, which is exactly the rHLB of OA, and isopropanol, were employed as the emulsifier and co-emulsifier to formulate OA NE. The size was about 41.37 ± 1.17 nm (Figure S2).

Shear-thinning (pseudoplastic) fluids exhibit low-viscosity fluid behavior when tested under high shear conditions, with zero flow under gravitational stress. This type of fluid is often demanded in the cosmetic and pharmaceutical industries.[44–46] All of the four NE presented shear-thinning behavior, implying the prosperous utility in industry. PAEE NE displayed higher viscosity with respect to PSO NE and PA-PSO NE. The possible explanation is that the polarity of PAEE was the lowest among the three oils, leading to the weaker interaction among PAEE, emulsifier and co-emulsifier. Consequently, PAEE NE had more chance to interplay with water and yielded higher viscosity. The interfacial storage modulus (G′) denotes the recoverable energy stored in the interface, which is related to the elasticity of NE. The loss modulus (G″) represents the loss energy during the shearing process.[47] The G″ of the four NE was significantly higher than G′, manifesting that the four NE belong to fluids with good mobility.

Owing to the low pH of the gastric fluid, the anions on the surface of the four NEs were neutralised by the cations, resulting in the charge reversal along with small absolute values of zeta potential.[48] However, except OA NE, other NE kept stable in gastric fluid, which may be attributed to their very small diameters. The presence of bile salts and free fatty acids from lipolysis in the intestinal fluid leads to an increase in the absolute zeta potential of the four NE.[49] The elevated net potentials hindered the assemble of the NE and enhanced their stability in intestinal fluid.

Due to the tight junctions and high membrane resistance, phenol red is limited in its paracellular migration in the intestinal epithelial monolayer. Phenol red does not penetrate into the mucosa and can be used as a non-absorbable labeling compound.[50–52] In this study, phenol red was used as an indicator to assess the small intestinal permeability. Various samples were incubated with mouse small intestine under 37 °C for 4 h, followed by being replaced with phenol red solution. The transport amount of phenol red across small intestines denoted the permeability of small intestine pre-treated with the samples. The results also show that pre-treating small intestines with PA-PSO and PAEE enhanced the

permeation of phenol red, suggesting that opening tight junctions is one mechanism for PA-PSO and PAEE to improve intestinal absorption.

The permeation of phenol red across intestinal membrane with PAEE and PA-PSO did not present a concentration-dependent mode. The highest permeation rate was obtained at 2.5% PAEE and 5% PA-PSO, respectively. The possible explanation is that as the oil concentration elevated, both the number and diameter of the emulsion droplets increased. Since the surface area of a droplet is inversely related to its size, the enlarged droplet had smaller surface area. For this reason, the total surface area of emulsions does not always ascend with oil concentration. When total surface area decreased, the contact area of emulsions with intestinal membrane diminished, leading to the reduced effect of emulsions on small intestines. We assume that compared to the other concentrations, 2.5% PAEE and 5% PA-PSO (v/v) may yield the emulsions with the largest total surface area, which account for the strongest permeability-prompting capacity. To verify our hypothesis, the intestinal fluid was used to dilute PSO, PA-PSO, PAEE, and OA, making the oil concentration amount to 2.5%, 5% and 10%, respectively. It confirms that the diameters of droplets indeed rose with the increment of oil concentration. Compared to 10% PSO and 10% OA, PA-PSO and PAEE of 10% (v/v) yielded larger emulsions after the incubation with intestinal fluid for 4 h, indicating that the total surface area of emulsions from 10% PA-PSO and 10% PAEE may decrease, which was responsible for their weakened strength on small intestines.

Contrary to our expectation, the permeation rate of phenol red with NE was only 50% to 70% that of the oil at optimal concentration. The possible reason is that NE is hydrophilic, while oil is hydrophobic. Since the small intestine is composed of lipid ingredients, the hydrophobic component may have more chance to interact with small intestine and change its permeability. It has been extensively reported that NE is capable of enhancing the solubility as well as bioavailability of the drugs with poor water solubility.[53–55] Our study demonstrates that improving intestinal permeability is not a primary contributing factor to the absorption-enhancing effect of NE. Other mechanisms, for example, increasing the contact area with small intestinal mucosa via the large surface area, boosting aqueous solubility of drugs, may be mainly responsible for the strength of NE.

PCA indicates that the oil with small rHLB possesses strong permeability-enhancing effect. Low rHLB indicates that the oil may have more potent affinity with lipophilic components. As intestinal mucosa consists of lipid constituents, the oil with low rHLB may yield more interaction with mucosa and increase its permeability. The permeability-prompting effect of NE was positively related to the viscosity and negatively correlated with zeta potential. High viscosity assists the NE to adhere to the intestinal mucosa and exert the permeation-prompting effect. As the mucosa carries negative charge, the NE with higher negative potential will be difficult to approach the mucosa, which weakens NE strength on mucosa.

In this study, the potential impairment of intestinal mucosa induced by absorption enhancers was estimated by assaying cytokine level, the enzyme activity of sucrase and MPO, as well as intestinal histomorphology observation. Sucrase, located in intestinal brush border, represents small intestinal absorption capacity that maintains relatively constant throughout life.[56] Sucrose was decomposed into glucose under the catalysis of sucrase. Glucose level stands for the activity of sucrase in small intestines. The oils from PA series did not bring obvious unfavorable impact on intestinal sucrase. The corresponding NE slightly decreased the sucrase activity, implying low toxicity on intestinal mucosa. The influence of vegetable oils and fatty acids on intestinal mucosa is different, depending on the variety of fatty acids. For example, alga oil could protect intestinal barrier from damage caused by antibiotic in mice.[57,58] Patchouli oil alleviated 5-fluorouracil-induced intestinal mucositis in rats.[59] Short chain, medium chain and polyunsaturated fatty acid showed therapeutic functions on intestinal inflammation of pigs.[60,61] On the other hand, Ghezzal found that short exposure to palmitic acid or palm oil impaired intestinal barrier integrity and triggered inflammation.[62] Kuratko reported that supplementing linoleic acid increased the activity of manganese superoxide dismutase, indicating the occurrence of intestinal chronic inflammation.[63] Our study demonstrates that the oils from PA series and their NE did not induce obvious inflammatory reactions, while OA and its NE triggered severe inflammation in small intestines. The side effect of OA was more serious than that of OA NE. OA combined α-lactalbumin in plasma and formed a toxic complex. Both the complex and free OA could trigger similar apoptotic mechanisms in tissue and initiated inflammation through the NF-kappa B and MAPK p38 signaling pathways.[64] Nevertheless, extra olive oil in which OA is the principal fatty acid and present in the form of triglycerides exhibited the therapeutic effect on the mice suffering from colitis by alleviating the

rectal bleeding and reducing the expression of inflammatory cytokines.[65] It implies that the carboxyl of OA may be responsible for its toxicity on intestines. Our study demonstrates that compared to OA and OA NE, the oils from PA series and their NE exhibited much lower toxicity on small intestine. In particular, PAEE and its NE did not show obvious damage toward intestinal mucosa. It has great potential to be utilized as food additive to enhance the absorption of nutrients. PAEE can also serve as an additive to be involved in various oral formulations, such as tablets, capsules, granules, and improve the oral bioavailability of drugs with poor membrane permeation.

Conclusion

PAEE was successfully synthesized, and its structure was confirmed by UV, IR, GC-MS, and NMR. PAEE significantly enhanced the stability of PA. Rheological test showed that the NE of OA and PA series was pseudoplastic fluid with good mobility. The effect of the oils in enhancing the permeability of small intestines was remarkedly stronger than that of the corresponding NE ($p < 0.05$). Meanwhile, the oils from PA series exhibited much more potent strength in increasing intestinal permeability than OA ($p < 0.05$). There was no obvious effect difference among PSO, PA-PSO and PAEE. The permeation-enhancing capacity of oils was negatively correlated with the oil density and rHLB, while the effect of NE was positively related to the viscosity and inversely correlated with the zeta potential. Meanwhile, the permeability-prompting strength of NE was irrespective with its oil phase. OA and OA NE brought severe inflammatory reaction in small intestines by damaging intestinal mucosa and villi after oral administration for 10 d. On the contrary, the oils from PA series and their NE exhibited much mild side effects. Moreover, PAEE and its NE presented protective effect on intestinal mucosa and maintained the smoothness of villus wall. The study suggests that PAEE is a promising absorption enhancer with excellent permeability-prompting and intestinal protection capacity against inflammation. Considering a lot of drugs have oral absorption obstacles, PAEE may hold promising perspectives in improving the therapeutic effects of oral drugs. However, long-term toxicity study needs to be conducted in the future to confirm the safety of PAEE and provide the substantial evidence for its clinical application.

Acknowledgments

Disclosure

The authors report no conflicts of interest in this work.

References

1. Markovic M, Zur M, Ragatsky I. et al. BCS class IV oral drugs and absorption windows: regional-dependent intestinal permeability of furosemide. *Pharmaceutics*. 2020;12(12):1175. doi:10.3390/pharmaceutics12121175

2. Öztürk-Atar K, Kaplan M, Çalış S. Development and evaluation of polymeric micelle containing tablet formulation for poorly water-soluble drug: tamoxifen citrate. *Drug Dev Ind Pharm*. 2020;46(10):1695–1704. doi:10.1080/03639045.2020.1820037

3. Maher S, Mrsny RJ, Brayden DJ. Intestinal permeation enhancers for oral peptide delivery. *Adv Drug Deliv Rev*. 2016;106(Pt B):277–319. doi:10.1016/j.addr.2016.06.005

4. Maher S, Brayden DJ, Casettari L, Illum L. Application of permeation enhancers in oral delivery of macromolecules: an update. *Pharmaceutics*. 2019;11(1):41. doi:10.3390/pharmaceutics11010041

5. Lakshminarayana R, Baskaran V. Influence of olive oil on the bioavailability of carotenoids. *Eur J Lipid Sci Technol*. 2013;115(10):1085–1093. doi:10.1002/ejlt.201200254

6. Nidhi B, Mamatha BS, Baskaran V. Olive oil improves the intestinal absorption and bioavailability of lutein in lutein-deficient mice. *Eur J Nutr*. 2014;53(1):117–126. doi:10.1007/s00394-013-0507-9

7. Yao HT, Lin JH, Liu YT, et al. Food-drug interaction between the adlay bran oil and drugs in rats. *Nutrients*. 2019;11(10):2473. doi:10.3390/nu11102473

8. Weerakoon WNMTDN, Anjali NVP, Jayathilaka N, et al. Soybean oil and coconut oil enhance the absorption of chlorogenic acid in humans. *J Food Biochem*. 2021;45:13823. doi:10.1111/jfbc.13823

9. Liu W, Zhao Q, Lv L, et al. Pomegranate seed oil enhances the percutaneous absorption of trans-resveratrol. *J Oleo Sci*. 2018;67(4):479–487. doi:10.5650/jos.ess17144

10. Özcan MM, Alkaltham MS, Uslu N, et al. Effect of different roasting methods on the bioactive properties, phenolic compounds and fatty acid compositions of pomegranate seed and oils. *J Food Sci Technol*. 2021;58(6):2283–2294. doi:10.1007/s13197-020-04739-1

11. Shabbir MA, Khan MR, Saeed M, et al. Punicic acid: a striking health substance to combat metabolic syndromes in humans. *Lipids Health Dis*. 2017;16(1):99. doi:10.1186/s12944-017-0489-3

12. Patil UK, Saraogi R. Natural products as potential drug permeation enhancer in transdermal drug delivery system. *Arch Dermatol Res*. 2014;306 (5):419–426. doi:10.1007/s00403-014-1445-y

13. Barichello JM, Morishita M, Takayama K, et al. Enhanced rectal absorption of insulin-loaded Pluronic F-127 gels containing unsaturated fatty acids. *Int J Pharm*. 1999;183(2):125–132. doi:10.1016/s0378-5173(99)00090-3

14. Espitia PJP, Fuenmayor CA, Otoni CG. Nanoemulsions: synthesis, characterization, and application in bio-based active food packaging. *Compr Rev Food Sci Food Saf*. 2019;18(1):264–285. doi:10.1111/1541-4337.12405

15. Yin J, Xiang C, Wang P, et al. Biocompatible nanoemulsions based on hemp oil and less surfactants for oral delivery of baicalein with enhanced bioavailability. *Int J Nanomed*. 2017;12:2923–2931. doi:10.2147/IJN.S131167

16. Sun D, Wei X, Xue X, et al. Enhanced oral absorption and therapeutic effect of acetylpuerarin based on D-α-tocopheryl polyethylene glycol 1000 succinate nanoemulsions. *Int J Nanomed*. 2014;9:3413–3423. doi:10.2147/IJN.S63777

17. Ferreira LM, Sari MHM, Cervi VF, et al. Pomegranate seed oil nanoemulsions improve the photostability and in vivo antinociceptive effect of a non-steroidal anti-inflammatory drug. *Colloids Surf B Biointerfaces*. 2016;144:214–221. doi:10.1016/j.colsurfb.2016.04.008

18. Lu LY, Liu Y, Zhang ZF, et al. Pomegranate seed oil exerts synergistic effects with trans-resveratrol in a self-nanoemulsifying drug delivery system. *Biol Pharm Bull*. 2015;38(10):1658–1662. doi:10.1248/bpb.b15-00371

19. Hashimoto Y, Tachibana K, Krug SM, et al. Potential for tight junction protein-directed drug development using claudin binders and angubindin-1. *Int J mol Sci*. 2019;20(16):4016. doi:10.3390/ijms20164016

20. Zou L, Zhang Z, Chen J, et al. β-cyclodextrin-grafted chitosan enhances intestinal drug absorption and its preliminary mechanism exploration. *AAPS Pharm Sci Tech*. 2022;23(6):221. doi:10.1208/s12249-022-02380-z

21. Nakaya Y, Takaya M, Hinatsu Y, et al. Enhanced oral delivery of bisphosphonate by novel absorption enhancers: improvement of intestinal absorption of alendronate by N-acyl amino acids and N-acyl taurates and their absorption-enhancing mechanisms. *J Pharm Sci*. 2016;105 (12):3680–3690. doi:10.1016/j.xphs.2016.09.004

22. Yang P, Yang X, Liu H, et al. Isolation of punicic acid from pomegranate seed oil by modified freeze crystallization and response surface methodology. *J Food Process*. 2022;46(12):e17154. doi:10.1111/jfpp.17154

23. Meher JG, Yadav NP, Sahu JJ, et al. Determination of required hydrophilic-lipophilic balance of citronella oil and development of stable cream formulation. *Drug Dev Ind Pharm*. 2013;39(10):1540–1546. doi:10.3109/03639045.2012.719902

24. Muszyńska B, Kała K, Sułkowska-Ziaja K, Krakowska A, Opoka W. Agaricus bisporus and its in vitro culture as a source of indole compounds released into artificial digestive juices. *Food Chem*. 2016;199:509–515. doi:10.1016/j.foodchem.2015.12.041

25. Yang P, Luo J, Yan S, et al. Permeation of hydroxypropyl-beta-cyclodextrin and its inclusion complex through mouse small intestine determined by spectrophotometry. *Curr Pharm Anal*. 2022;18(2):199–207. doi:10.2174/1573412917666210329145917

26. Yin H, Pan X-C, Wang S-K, et al. Protective effect of wheat peptides against small intestinal damage induced by non-steroidal anti-inflammatory drugs in rats. *J Integr Agric*. 2014;13(9):2019–2027. doi:10.1016/S2095-3119(13)60619-X

27. Menozzi A, Pozzoli C, Poli E, et al. Diazoxide attenuates indomethacin-induced small intestinal damage in the rat. *Eur J Pharmacol*. 2011;650 (1):378–383. doi:10.1016/j.ejphar.2010.09.078

28. Zhang CY, Lin X, Feng B, et al. Enhanced leavening properties of baker's yeast by reducing sucrase activity in sweet dough. *Appl Microbiol Biotechnol*. 2016;100(14):6375–6383. doi:10.1007/s00253-016-7449-0

29. Olfert M, Bäurer S, Wolter M, et al. Comprehensive profiling of conjugated fatty acid isomers and their lipid oxidation products by two-dimensional chiral RP×RP liquid chromatography hyphenated to UV- and SWATH-MS-detection. *Anal Chim Acta*. 2022;1202:339667. doi:10.1016/j.aca.2022.339667

30. Van Nguyen A, Deineka V, Deineka L, et al. Comparison of separation of seed oil triglycerides containing isomeric conjugated octadecatrienoic acid moieties by reversed-phase HPLC. *Separations*. 2017;4(4):37. doi:10.3390/separations4040037

31. Smith BC. The C=O bond, Part III: carboxylic acids. *Spectroscopy*. 2018;33(1):14–20.

32. Paczkowska M, Mizera M, Dzitko J, et al. Vibrational (FT-IR, Raman) and DFT analysis on the structure of labile drugs. The case of crystalline tebipenem and its ester. *J Mol Struct*. 2017;1134(15):135–142. doi:10.1016/j.molstruc.2016.12.074

33. Yarnall YY, Hudson RL. Infrared intensities of methyl acetate, an interstellar compound - comparisons of three organic esters. *Spectrochim Acta A*. 2022;283(15):121738. doi:10.1016/j.saa.2022.121738

34. Kaufman M, Wiesman Z. Pomegranate oil analysis with emphasis on MALDI-TOF/MS triacylglycerol fingerprinting. *J Agric Food Chem*. 2007;55 (25):10405–10413. doi:10.1021/jf072741q

35. Anh NV, Victor D, Anh VTN, et al. *Thladiantha* Seed Oils - New Source of Conjugated Fatty Acids: characterization of Triacylglycerols and Fatty Acids. *J Oleo Sci*. 2020;69(9):993–1000. doi:10.5650/jos.ess20075

36. Cao Y, Yang L, Gao HL, et al. Re-characterization of three conjugated linolenic acid isomers by GC-MS and NMR. *Chem Phys Lipids*. 2007;145 (2):128–133. doi:10.1016/j.chemphyslip.2006.11.005

37. Wu WX, Qu L, Liu BY, et al. Lipase-catalyzed synthesis of acid-degradable poly(β-thioether ester) and poly(β-thioether ester-co-lactone) copolymers. *Polymer*. 2015;59(24):187–193. doi:10.1016/j.polymer.2015.01.002

38. Martin-Piñero MJ, Muñoz J, Alfaro-Rodriguez M-C. Improvement of the rheological properties of rosemary oil nanoemulsions prepared by microfluidization and vacuum evaporation. *J Ind Eng Chem*. 2020;91:340–346. doi:10.1016/j.jiec.2020.08.018

39. Davis JP, Sweigart DS, Price KM, et al. Refractive index and density measurements of peanut oil for determining oleic and linoleic acid contents. *J Am Oil Chem Soc*. 2013;90(2):199–206. doi:10.1007/s11746-012-2153-4

40. Amat Sairin M, Abd Aziz S, Yoke Mun C, et al. Analysis and prediction of the major fatty acids in vegetable oils using dielectric spectroscopy at 5–30 MHz. *PLoS One*. 2022;17(5):e0268827. doi:10.1371/journal.pone.0268827

41. Lee YY, Yoon KS. Determination of required HLB values for citrus unshiu fruit oil, citrus unshiu peel oil, horse fat and camellia japonica seed oil. *J Cosmet Sci*. 2020;71(6):411–424.

42. De Lima Cherubim DJ, Buzanello Martins CV, Oliveira Fariña L, et al. Polyphenols as natural antioxidants in cosmetics applications. *J Cosmet Dermatol*. 2020;19(1):33–37. doi:10.1111/jocd.13093

43. Tian M, Bai Y, Tian H, et al. The chemical composition and health-promoting benefits of vegetable oils-a review. *Molecules*. 2023;28(17):6393. doi:10.3390/molecules28176393

44. Eid AM, Issa L, Al-Kharouf O, et al. Development of Coriandrum sativum Oil Nanoemulgel and Evaluation of Its Antimicrobial and Anticancer Activity. *Biomed Res Int*. 2021;2021(1):5247816. doi:10.1155/2021/5247816

45. Syed Azhar SNA, Ashari SE, Salim N. Development of a kojic monooleate-enriched oil-in-water nanoemulsion as a potential carrier for hyperpigmentation treatment. *Int J Nanomed*. 2018;13:6465–6479. doi:10.2147/IJN.S171532

46. Arshad T, Shoaib Khan HM, Akhtar N, et al. Structural elucidation and development of azelaic acid loaded mesoporous silica nanoparticles infused gel: revolutionizing nanodrug delivery for cosmetics and pharmaceuticals. *Heliyon*. 2024;10(8):e29460. doi:10.1016/j.heliyon.2024.e29460

47. Artiga-Artigas M, Reichert C, Salvia-Trujillo L, et al. Protein/polysaccharide complexes to stabilize decane-in-water nanoemulsions. *Food Biophys*. 2020;15(3):335–345. doi:10.1007/s11483-019-09622-x

48. Singh H, Ye A, Horne D. Structuring food emulsions in the gastrointestinal tract to modify lipid digestion. *Prog Lipid Res*. 2009;48(2):92–100. doi:10.1016/j.plipres.2008.12.001

49. Salvia-Trujillo L, Qian C, Martín-Belloso O, et al. Influence of particle size on lipid digestion and β-carotene bioaccessibility in emulsions and nanoemulsions. *Food Chem*. 2013;141(2):1472–1480. doi:10.1016/j.foodchem.2013.03.050

50. Liu Z, An T, Yuan R, et al. Comparison of the phenol red, gravimetric, and synthesized mPEG-PR methods for correcting water flux using the single-pass intestinal perfusion method. *Eur J Pharm Sci*. 2022;176:106255. doi:10.1016/j.ejps.2022.106255

51. Soyseven M, Kaynak MS, Çelebier M, et al. Development of a RP-HPLC method for simultaneous determination of reference markers used for in-situ rat intestinal permeability studies. *J Chromatogr B Analyt Technol Biomed Life Sci*. 2020;1147:122150. doi:10.1016/j.jchromb.2020.122150

52. Chen G, Min X, Zhang Q, et al. Synthesis and evaluation of PEG-PR for water flux correction in an In situ rat perfusion model. *Molecules*. 2020;25(21):5123. doi:10.3390/molecules25215123

53. Jha SK, Han HS, Subedi L, et al. Enhanced oral bioavailability of an etoposide multiple nanoemulsion incorporating a deoxycholic acid derivative-lipid complex. *Drug Deliv*. 2020;27(1):1501–1513. doi:10.1080/10717544.2020.1837293

54. Anuar N, Sabri AH, Bustami Effendi TJ, et al. Development and characterisation of ibuprofen-loaded nanoemulsion with enhanced oral bioavailability. *Heliyon*. 2020;6(7):e04570. doi:10.1016/j.heliyon.2020.e04570

55. Babadi D, Dadashzadeh S, Osouli M, et al. Biopharmaceutical and pharmacokinetic aspects of nanocarrier-mediated oral delivery of poorly soluble drugs. *J Drug Delivery Sci Technol*. 2021;62:102324. doi:10.1016/j.jddst.2021.102324

56. Clarke JM, Pelton NC, Bajka BH, et al. Use of the ^{13}C-sucrose breath test to assess chemotherapy-induced small intestinal mucositis in the rat. *Cancer Biol Ther*. 2006;5(1):34–38. doi:10.4161/cbt.5.1.2235

57. Zhang H, Xu Z, Chen W, et al. Algal oil alleviates antibiotic-induced intestinal inflammation by regulating gut microbiota and repairing intestinal barrier. *Front Nutr*. 2023;9:1081717. doi:10.3389/fnut.2022.1081717

58. Yang C, Qiao Z, Xu Z, et al. Algal oil rich in docosahexaenoic acid alleviates intestinal inflammation induced by antibiotics associated with the modulation of the gut microbiome and metabolome. *J Agric Food Chem*. 2021;69(32):9124–9136. doi:10.1021/acs.jafc.0c07323

59. Gan Y, Ai G, Wu J, et al. Patchouli oil ameliorates 5-fluorouracil-induced intestinal mucositis in rats via protecting intestinal barrier and regulating water transport. *J Ethnopharmacol*. 2020;250:112519. doi:10.1016/j.jep.2019.112519

60. Liu Y. Fatty acids, inflammation and intestinal health in pigs. *J Anim Sci Biotechnol*. 2015;6(1):41. doi:10.1186/s40104-015-0040-1

61. Sundaram TS, Giromini C, Rebucci R, et al. Role of omega-3 polyunsaturated fatty acids, citrus pectin, and milk-derived exosomes on intestinal barrier integrity and immunity in animals. *J Anim Sci Biotechnol*. 2022;13(1):40. doi:10.1186/s40104-022-00690-7

62. Ghezzal S, Postal BG, Quevrain E, et al. Palmitic acid damages gut epithelium integrity and initiates inflammatory cytokine production. *Biochim Biophys Acta mol Cell Biol Lipids*. 2020;1865(2):158530. doi:10.1016/j.bbalip.2019.158530

63. Kuratko CN, Constante BJ. Linoleic acid and tumor necrosis factor-alpha increase manganese superoxide dismutase activity in intestinal cells. *Cancer Lett*. 1998;130(1–2):191–196. doi:10.1016/s0304-3835(98)00136-0

64. Chetta KE, Alcorn JL, Baatz JE, et al. Cytotoxic lactalbumin-oleic acid complexes in the human milk diet of preterm infants. *Nutrients*. 2021;13(12):4336. doi:10.3390/nu13124336

65. Cariello M, Contursi A, Gadaleta RM, et al. Extra-virgin olive oil from apulian cultivars and intestinal inflammation. *Nutrients*. 2020;12(4):1084. doi:10.3390/nu12041084